buildings

MDPI

Article

Design Model of Rectangular Concrete-Filled Steel Tubular Stub Columns under Axial Compression

Faesal Alatshan [1,2], Siti Aminah Osman [1,*], Abdelmajeed Altlomate [3], Mohammed Alkair [2], Roszilah Hamid [1] and Fidelis Mashiri [4]

[1] Department of Civil Engineering, Universiti Kebangsaan Malaysia (UKM), Bangi 43600, Selangor, Malaysia
[2] Civil Engineering Department, College of Engineering Technology, Houn P.O. Box 61160, Libya
[3] Department of Civil Engineering, Faculty of Civil Engineering, Sirte University, Sirte P.O. Box 61160, Libya
[4] School of Engineering, Design and Built Environment, Western Sydney University, Kingswood, NSW 2747, Australia
* Correspondence: saminah@ukm.edu.my

Abstract: This research collected and summarized a total of 455 experimental tests of axially loaded square and rectangular concrete-filled steel tubular (CFST) stub columns. The recently published papers were used to evaluate the current design equations from four international standards, namely the American Concrete Institute (ACI) code, British Standard (BS5400), Chinese standard (BDJ13-51), and Eurocode 4 (EC4). It was found that the results obtained from the codes have appreciable differences and could be improved, especially for the specimens fabricated using high-resistance materials. Therefore, new empirical equations were proposed based on the four standard formulas and the wide range of previously available experimental data to provide more accurate estimations. The proposed equations could predict an average sectional capacity of only 0.1% lower than the experimental results, with better data scattering than the existing equation's results.

Keywords: concrete-filled steel tubular (CFST); axial load; square; rectangular; column; empirical; compression; standards

check for updates

Citation: Alatshan, F.; Osman, S.A.; Altlomate, A.; Alkair, M.; Hamid, R.; Mashiri, F. Design Model of Rectangular Concrete-Filled Steel Tubular Stub Columns under Axial Compression. *Buildings* **2023**, *13*, 128. https://doi.org/10.3390/buildings13010128

Academic Editors: Wee Teo, Ehsan Jarghouyeh and Bo Yang

Received: 8 October 2022
Revised: 24 November 2022
Accepted: 16 December 2022
Published: 4 January 2023

Copyright: © 2023 by the authors. Licensee MDPI, Basel, Switzerland. This article is an open access article distributed under the terms and conditions of the Creative Commons Attribution (CC BY) license (https://creativecommons.org/licenses/by/4.0/).

1. Introduction

Concrete-filled steel tubular (CFST) elements were employed in the construction industry in the early 1900s. Nevertheless, the research investigations in CFST elements did not begin until the early 1960s. After that, many research studies were conducted to understand the behavior of CFST elements. Concrete-filled steel tubular (CFST) structures are increasing in popularity in many engineering applications, including high-rise buildings, bridge structures, supporting platforms of offshore structures and piles. As a consequence of its composite effects, the disadvantages of the two materials can be compensated for, and their advantages in CFST can be combined to provide efficient structural systems. CFST elements have the advantage of high mechanical strength, increased fire resistance, appropriate durability, energy absorption during earthquakes, and no formwork is needed compared to other concrete-steel composite structural elements. The core concrete works to prevent the steel tube from buckling inward. Meanwhile, the confinement of core concrete by the steel tube works to strengthen the mechanical properties of concrete. Consequently, adopting CFST columns results in a relatively small cross-sectional area with considerable economic savings [1–3].

CFSTs with regular cross-sections, such as circular, square and rectangular shapes, have been widely investigated [4], yet some research has been conducted on other cross-sectional shapes, for example, Chang et al. [5] conducted an experimental and numerical study to investigate the static axial performance of stiffened concrete-filled double-skin steel tubular (CFDST) stub columns with circular and square shapes. In addition, Rahnavard et al. [6,7] conducted experimental and numerical analysis on four different cross-section shapes of

fabricated concrete-filled cold-formed steel (CF-CFS) short and long columns. For both long and short columns, it was found that the ultimate strengths of the concrete-filled columns were higher than that of hollow columns. This was attributed to the concrete's role in resisting the buckling deformation of the steel sections. In addition, the results revealed that columns with square sections showed a higher load resistance than that of rectangular section columns. Not only the static behavior, but the seismic, impact, and blast performance of CFST elements has also been widely examined using different shapes and material strength, and the enhancement of the seismic behavior was clearly demonstrated by filling the columns with concrete [8,9].

Previous studies showed the complexity of the interaction relationship between the steel tube and the concrete core of the circular and rectangular CFST columns, during the various loading stages [10,11]. Meanwhile, it is well known that the performance of CFST circular cross-sections is better than square and rectangular sections in terms of concrete confinement and local buckling. Nevertheless, the square and rectangular sections are still increasingly utilized. These sections are easier to connect to other structural elements and have high bending stiffness and architectural appeal [1,12]. There are various modes of failure for the CFSTs depending on their material properties and geometric structure. Compared with the conventional type of concrete columns, the failure in the CFST column is delayed due to concrete confinement by the steel tube. Many other factors may affect the load-carrying capacity of the CFST column, which include cross-sectional shape, width-to-thickness ratio, and steel ratio. These parameters need to be re-investigated and compared with the wide range of available experimental results that have been carried out over the past few decades to improve the existing design equations and provide more accurate predictions.

Previously, a wide range of research efforts have been devoted to investigating the performance of CFST stub columns and have been compared with the design codes or with their own theoretical or numerical models [1,4]. These previous models typically exhibited good agreement with the experiments, particularly with the results used to develop the model, but it is unclear whether they will be able to make more accurate predictions than other experimental results. In other words, limited investigations have been carried out based on or to complement other researchers' test results; nevertheless, looking at the full research picture is necessary so that conclusions are not drawn based on the very limited results of a limited number of research investigations.

Therefore, in this study, a comprehensive database was established to summarize the previous experimental results of square and rectangular CFST stub columns tested under axial compression. The database was employed to evaluate the applicability of the methods described by several international standards to predict the axial load capacity and propose more accurate design models. In addition, it is hoped that the new database will help researchers to compare their hypotheses with these comprehensive findings to achieve the best possible balance between the cost and safety of square and rectangular CFST stub columns.

2. Summary of the Test Database

A database consisting of 455 experimental CFST rectangular and square stub columns subjected to axial compression was collected from various experimental studies carried out by past researchers. A database of different shapes of CFSTs collected by Goode et al. [13] has been utilized in this study. The database summarizes a series of tests on 1819 CFST columns subjected to various types of load conditions. A total of 313 rectangular and square CFST stub columns were obtained from this database to be used in the study. To increase the range of the experimental data, 142 tests of CFST stub columns were also compiled from the other previous investigations. These are: Lam and Gardner, 2008 [14]; Ellobody and Young, 2006 [15]; Zhang et al., 2005 [16]; Uy et al., 2011 [17]; Sakino, 2004 [18]; Wang et al., 2014 [19]; Shakir-Khalil and J Zeghiche, 1989 [20]; Shakir-Khalil and M Moul, 1990 [21].

The following inclusion and exclusion criteria were used to set the boundaries for the database:

1. The columns considered must be tested under static axial compression loads.
2. The columns must have square or rectangular single-skin cross-sections.
3. The concrete core and the steel tube must be loaded simultaneously, as illustrated in Figure 1.
4. The column specimens were checked to ensure that they can be classified as short columns according to the EC4 in which L/b $\leq$ 4; where L is the specimen length and b is the section width [22].
5. Irrelevant CFST columns made of different materials such as stainless steel or aluminum were excluded.
6. The columns should not have internal steel reinforcements, shear connectors, or any types of stiffeners, etc.

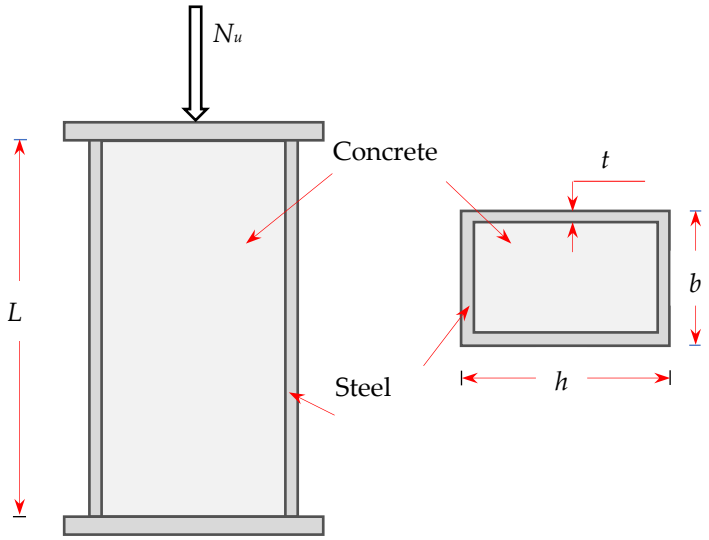


Figure 1. Test specimens.

The details of the collected test specimens in this new database are shown in Table A1, Appendix A.

Based on the wide range of specimens presented in the current database, Figure 2 displays a schematic view of the failure mechanism of rectangular CFST stub columns. It is well known that hollow steel columns exhibit both inward and outward buckling when subjected to axial loading, while as illustrated in Figure 2, only outward buckling occurs at the mid-height of concrete-filled steel tubular stub columns. This failure pattern is due to the support by concrete infill to the steel tube. Additionally, the presence of the steel tube around the concrete provides a confinement effect that delays the failure of the concrete core and makes it in a more ductile fashion. This interaction between the steel and concrete enhances the ultimate capacity of such columns compared to their counterparts of hollow steel tubes and reinforced concrete columns.

The range and distribution of the database contents concerning the geometric details, material strengths, and ultimate strengths are presented in Figure 3. It can be seen that the concrete strengths (f'_c) of the database specimens range from 15 MPa to 120 MPa, and most of them have a value of f'_c between 30 and 50 MPa. Additionally, the yield strength of the steel tube (f_y) varies from 180 MPa to 840 MPa and mostly ranged between 180 and 300 MPa. The confinement factor [$\xi = (A_s f_y)/(A_c f'_c)$] is distributed between 0.2 and 10.5. Additionally, most of the included specimens have a steel ratio [$\rho = A_s/A_c$] between 2% and 20%, while just a few specimens have a larger ratio. The column width-to-steel thickness ratio (b/t) ranged from 10 to 135. The ultimate section capacity (N_u) varied from 190 to 15,000 KN.

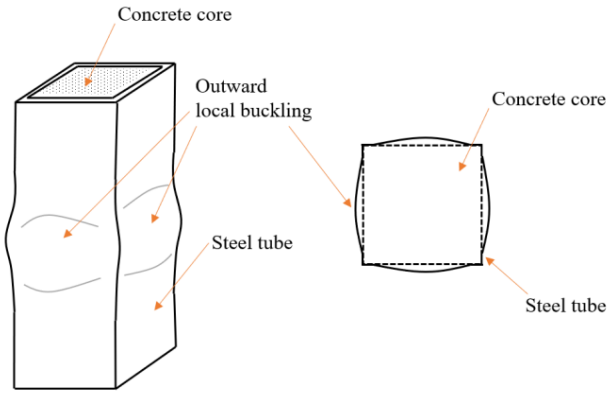


Figure 2. Schematic failure modes of rectangular CFST columns.

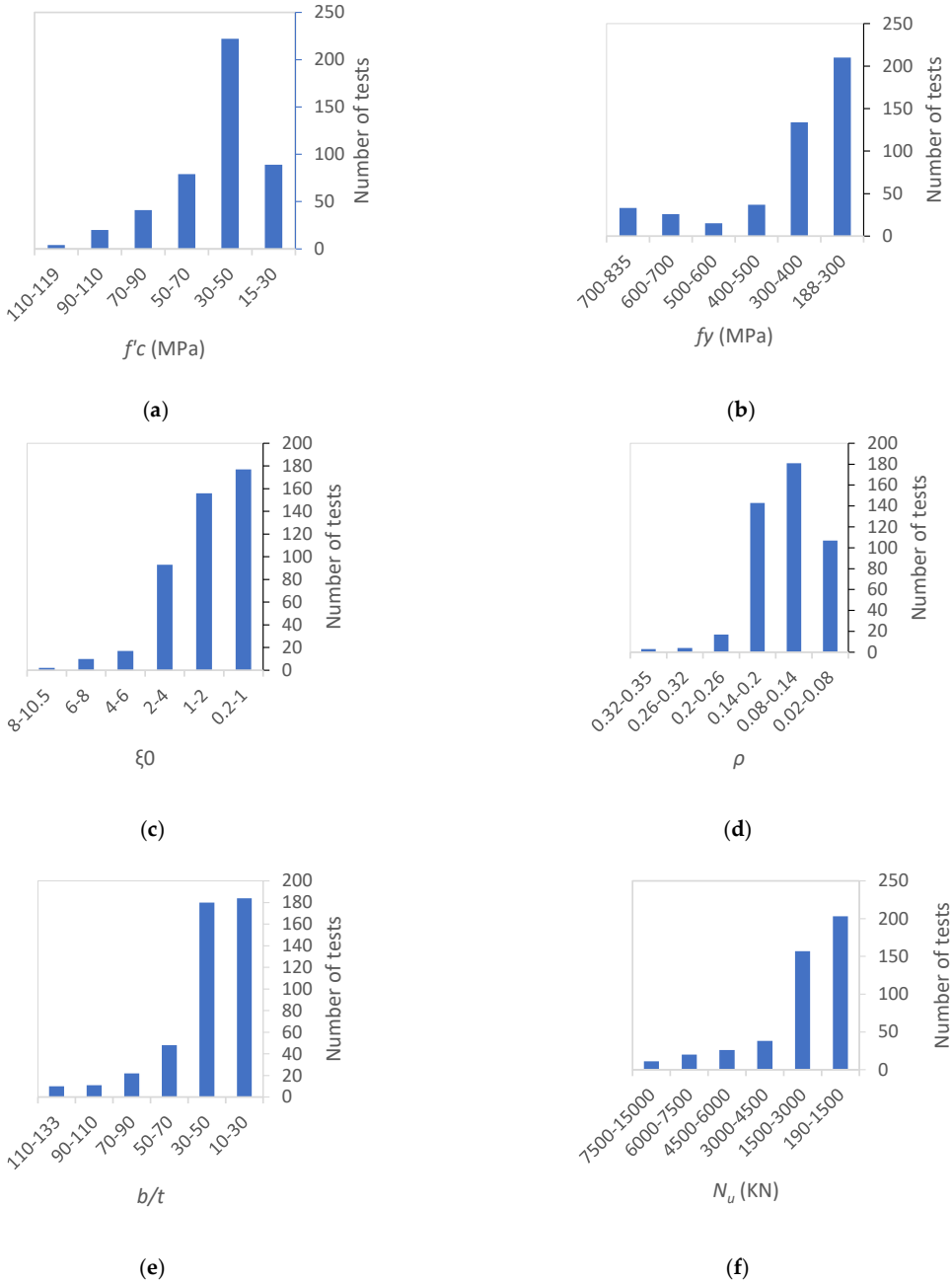


Figure 3. Distribution of test database in terms of (**a**) concrete strength, (**b**) steel strength, (**c**) confinement factor, (**d**) steel ratio, (**e**) width-to-steel thickness ratio and (**f**) ultimate section capacity.

Finally, all the specimens were such that the width (b) was from 50 mm to 324 mm, the height was from 100 mm to 2400 mm, and the steel thickness was from 1.2 mm to 9.7 mm. The details of the columns are provided in Table A1, Appendix A.

The compressive strength of concrete can be defined using different test methods depending on the standards used. Therefore, the Eurocode 2 standards [23] were used to convert between f'_c and f_{cu} [23], where f'_c is the compressive strength of concrete obtained from 150 × 300 mm cylinder specimens, and f_{cu} is the compressive strength of concrete obtained from a 150 mm cube.

3. Formulations of Current Design Codes

Different design codes provide different formulae for estimating and designing CFST stub columns under axial compression. Generally, the fundamental difference lies in the methods of determining the compressive strength of concrete. Four approaches from different international standards used in the United States, Japan, Europe, and China were compared to the results of the previously available data.

3.1. ACI Approach

The approach used to design the reinforced concrete sections has been adopted to calculate the axial capacity of CFST stub columns. American Concrete Institute ACI code [24] utilizes the same formulae for different cross-sections and does not consider the confinement effect.

The compressive capacity of CFST rectangular stub columns can be determined using Equation (1) according to the ACI code. A_s is shown in Equation (1), the design load based on ACI (NACI) is the summation of the ultimate axial sectional capacities of the concrete core and steel tube.

$$N_{ACI} = A_s f_y + 0.85\ A_c\ f_c \tag{1}$$

where, A_s is the cross-sectional area of RHS steel, Ac is the cross-sectional area of the concrete infill.

The same approach was also adopted by the Architectural Institute of Japan (AIJ) [25] guidelines to predict the CFST stub column strength for square and rectangular hollow sections.

3.2. EC4 Approach

Australian standard (AS5100) [26] and Eurocode 4 [22] use the same formula, see Equation (2), to determine the section compressive capacity of CFST RHS stub columns. Similar to the ACI code approach, the EC4 design load capacity (N_{EC4}) is calculated by summing up the section capacities of the concrete core and steel tube. However, the long-term effects are not considered.

$$N_{EC4} = A_s f_y + A_c f_c \tag{2}$$

3.3. BS5400 Approach

Equation (3) is used by British standards (BS5400) [27] to predict the capacity of CFST short columns under axial compression. Equation (3) is similar to the EC4 formula. However, the British standard utilizes 15 × 15 × 15 cm concrete cubes to determine the compressive strength of concrete.

$$\mathrm{N}_{BS} = A_s f_y + A_c f_{cu} \tag{3}$$

3.4. DBJ13-51 Approach

A different approach is recommended by the Chinese standard (DBJ13-51) [28] to predict the load-carrying capacity of CFST stub columns. The standard takes concrete confinement by the steel tube into account by introducing the confinement factor (ξ_0).

$$N_{DBJ} = (A_s + A_c)\ \ (1.18 + 0.85\ \ \xi_0) f_{ck} \tag{4}$$

$$\xi_0 = \frac{A_s\, f_y}{A_c\, f_{ck}} \tag{5}$$

where f_{ck} is the characteristic cube compressive strength of concrete, and Equation (6) was used as a conversion relationship between f_{ck} and f_{cu} [1].

$$f_{ck} = 0.67\, f_{cu} \tag{6}$$

3.5. Limitations of Current Design Codes

Despite the growing improvement in the properties of steel and concrete, international standards still limit the possibility of using very high-strength materials in CFST elements. For example, according to the Australian standard (AS/NZS 3678) [29], the limit values of yield stress (f_y) for both steel plates and cold-formed tubes should be between 200 and 450 MPa. For the steel plates, hot-rolled and cold-formed tubes, the European standard (EN 10025) [30] and the Chinese standard (GB50017) [31] suggest different yield stress (f_y) limits between 215 to 460 and 235 to 420 MPa, respectively. However, as shown in Figure 3b, in the newly proposed database, the yield strength of the steel tube (f_y) ranged from 180 MPa to 840 MPa, and the value of f_y mostly ranged between 180 and 300 MPa.

Different limitations of concrete compressive strength were also suggested in the international standards. In both AS5110 and EC4, the characteristic compressive cylinder strength at 28 days (f'_c) ranges between 25 to 65 MPa and between 20 to 60 MPa, respectively. In BS5400 and DBJ13-51, the characteristic cube compressive strength at 28 days (f_{cu}) should not be less than 20 and 30 MPa, respectively. While, as shown in Figure 3, the data of the existing experimental studies used in the proposed database covered a more comprehensive range of concrete strengths (f'_c) from 15 MPa to 120 MPa (f_{cu} ranges from 19 to 140).

This paper aims to participate in extending the limits allowed by the current design methods and suggests more comprehensive formulations.

3.6. Comparative Studies

In this section, the existing experimental results collected in the proposed database were compared with the predicted results using the previously mentioned international standards. This comparison was conducted to evaluate the applicability and accuracy of the standards. Figure 4 illustrates the relationship between the experimental and the predicted values of CFST short-column load-carrying capacity. Figure 4 also shows the mean, defined as the average ratio of the predicted capacity to the experimental strength, and the standard deviation (SD) of the ratio of the predicted capacity to the experimental strength. In this figure, the orange line shows the ideal results when the empirical results are identical to the experimental results. In other words, the further away the points are from this line means that they are more scattered and far from the correct results.

In general, and as expected, the predicted load-carrying capacities from the four codes have nearly the same trends compared to the experimental results. The BS5400 approach overestimates the capacity by 4% compared to the experimental data, while all other approaches underestimate the capacity. For instance, the DBJ13-51 approach predicts sectional capacities 2.8% lower than the experimental results, which have the most reliable mean value of predicted load-carrying capacity compared to the experimental results. However, the scatter of DBJ13-51 approach estimations is relatively high (SD = 0.142). The most faultless scatter was achieved by the ACI approach with standard deviations (SD) of 0.129, while the mean value was relatively higher at 13% lower than the experimental results. For the BS5400 and EC4 approaches, the standard deviation values of the predicted sectional capacities to the experimental results were 0.165 and 0.141, respectively. In light of these results, it can be seen that adjustments are required to make the standard predictions more accurate. These adjustments are discussed in the following sections.

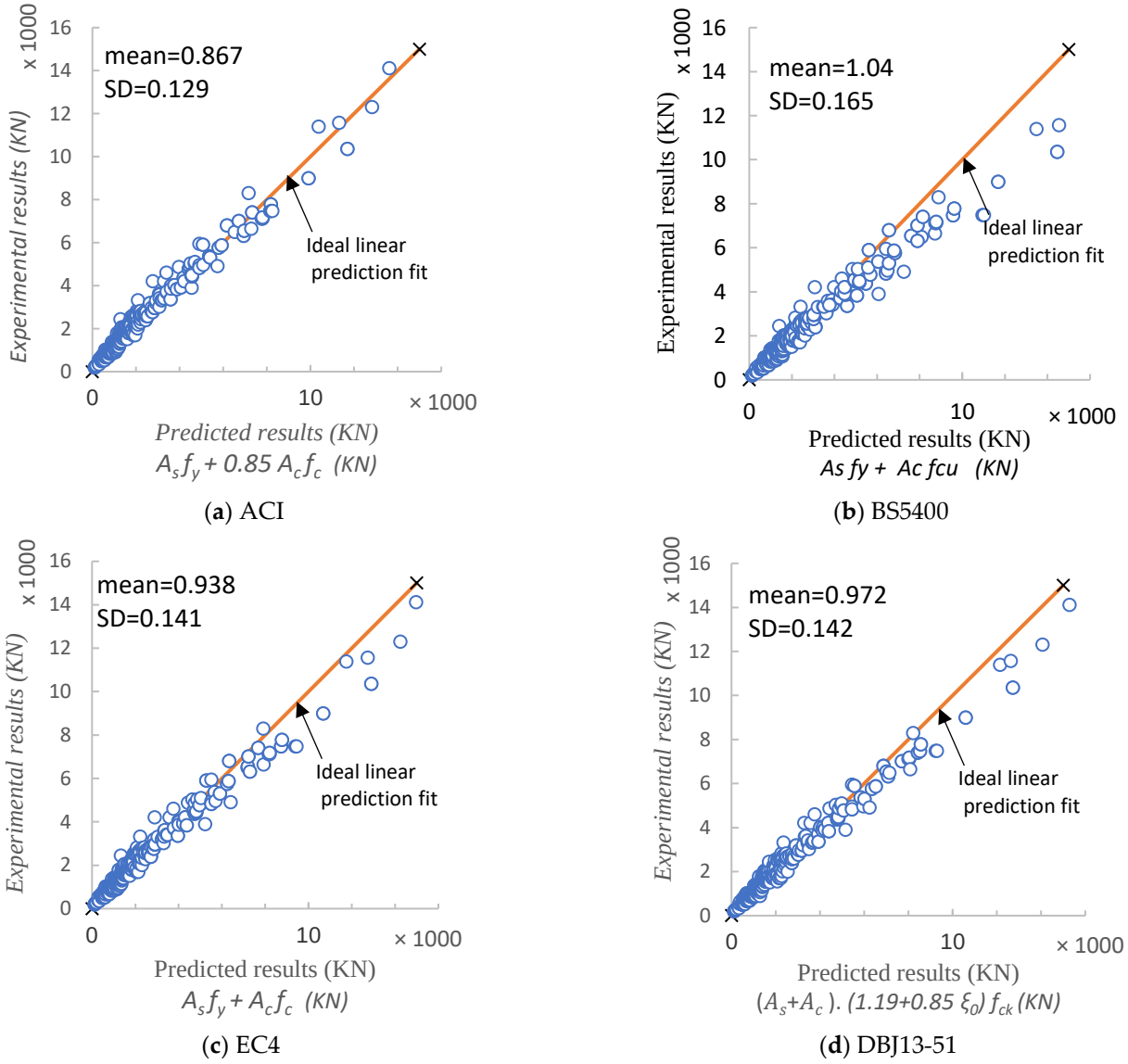


Figure 4. Comparison of the carrying capacity predictions of the different formulations.

4. New Design Models

In this section, two proposed approaches will be introduced to improve the existing equations to predict the load-carrying capacity of the CFST stub columns. The existing formulae were modified using correction factors to improve the mean, standard deviations, and variation coefficient (COV) of the results. The new proposed formulae were determined through regression analysis based on the 455 experimental tests.

4.1. The First Proposal to Modify the Existing Design Formulas

The same approach adopted by Lu and Zhao [32] and Hanoon et al. [33] has been used in this study. In order to improve the available equations for predicting the load axial carrying capacity of square and rectangular CFST stub columns. Some conditions are considered:

1. The equations must epitomize the experimental data as much as possible.
2. The expressions have to be similar to the existing expressions provided by the standards.
3. The formulae should be as simple as possible.

In the first design proposal, new correction coefficients (C1 and C2) were identified to develop the existing equations by improving the mean, standard deviations, and co-

efficient of variation. These new correction factors were introduced because the original equations described in Section 3 were originally proposed for the conventional column design. Whereas, these equations do not take into account the additional cross-sectional capacity increase due to the confinement effect provided by the steel tube to the concrete core of the CFST stub columns.

A programming code using Microsoft Excel VBA (Visual Basic for Applications) programing language was developed and used to calculate the correction coefficients of the first proposed equations. Figures 5 and 6 illustrate the flowcharts of the algorithm used to design this programming code. As illustrated, the regression analysis approach was employed to correct the prediction for the stub columns based on the 455 experimental tests.

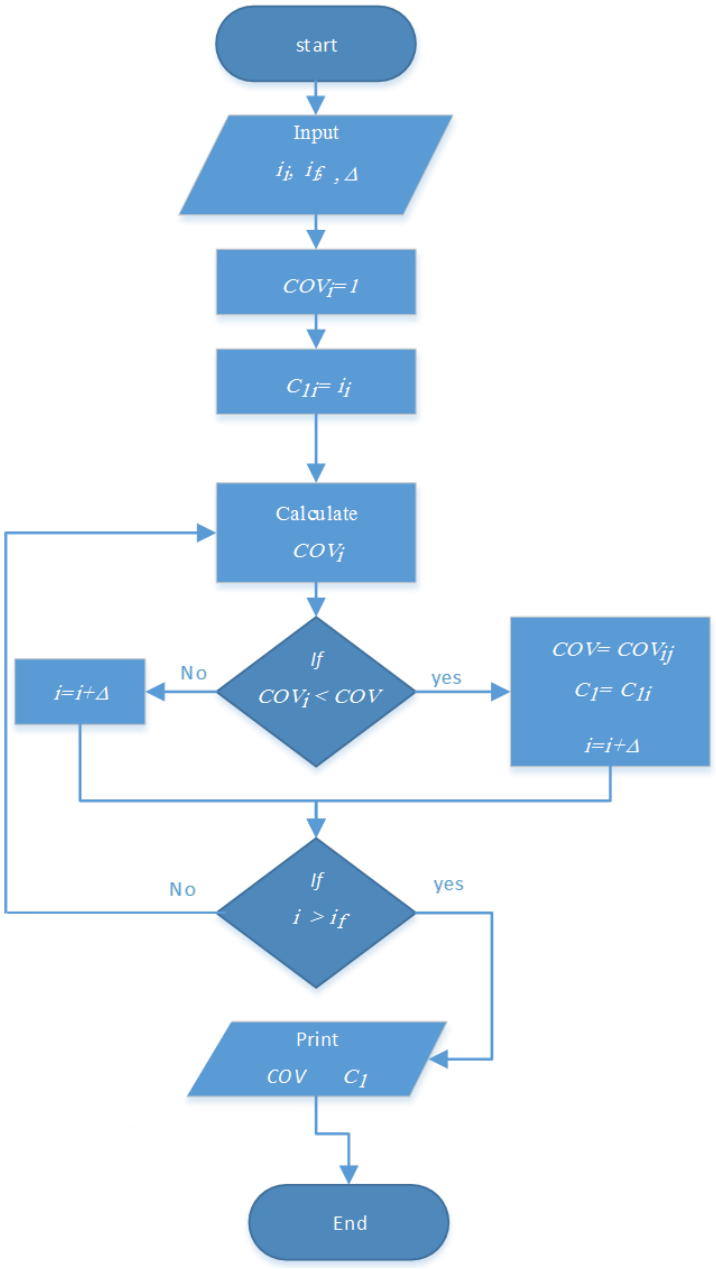


Figure 5. ACI first proposal flowchart.

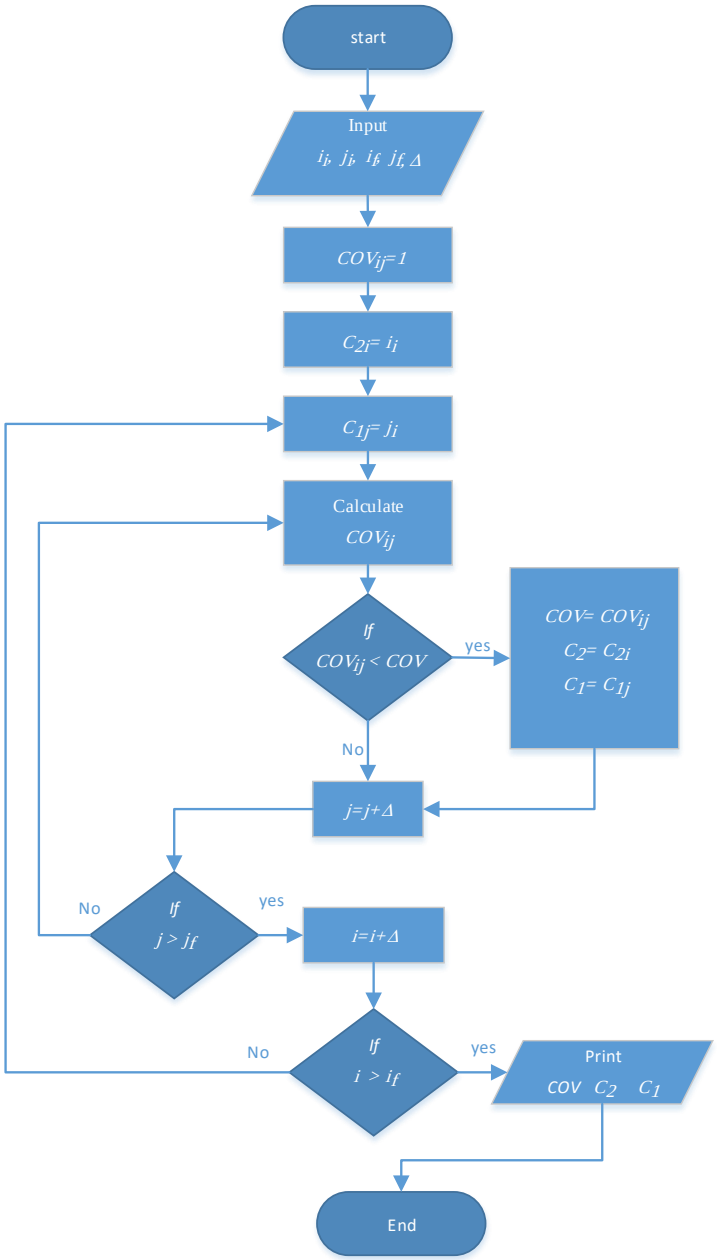


Figure 6. BS5400, EC4 and DBJ13-51 first proposal flowchart.

For the ACI code formula, and as illustrated in Equations (7) and (8), only one coefficient (C1) was targeted to be obtained to adjust the concrete capacity in the formula. At the same time, the steel section capacity (C2) was not modified and was assumed to be 1, as proposed in the code (Equation (1)).

$$C2 \text{ (Steel capacity)} + C1 \text{ (Concrete capacity)} \quad (7)$$

$$A_s f_y + C1\, A_c f'_c \qquad \text{ACI} \quad (8)$$

For the BS5400 and EC4 formulae, two coefficients (C1 and C2) were targeted to be found to adjust the concrete and steel capacity in the formulae.

$$C1\, A_s f_y + C2\, A_c f_{cu} \qquad \text{BS5400} \quad (9)$$

$$C1\, A_s f_y + C2\, A_c f'_c \qquad \text{EC4} \quad (10)$$

For the DBJ13-51 formula, due to the difference in the structure of the equations, two different coefficients (C1 and C2) have been targeted to adjust the formula, as shown in Equation (11).

$$(A_s + A_c)\cdot(C1 + C2\cdot\xi_0)\cdot f_{ck} \quad (11)$$

For all codes, the initial (i_i) and final (i_f) values of the concrete and steel coefficients (C1 and C2) were taken as 0.1 and 5, respectively, and the accuracy of C1 and C2 (Δ) was taken as 0.01.

The first proposal of the modified formula for the four different codes can be expressed as:

$$A_s f_y + 0.86\, A_c f'_c \quad (\text{KN}) \quad \text{ACI} \quad (12)$$

$$1.01\, A_s f_y + 0.92\, A_c f_{cu} \quad (\text{KN}) \quad \text{BS5400} \quad (13)$$

$$1.1\, A_s f_y + 0.92\, A_c f'_c \quad (\text{KN}) \quad \text{EC4} \quad (14)$$

$$(A_s + A_c)\, 1.19 + 0.85\, \xi_0 \quad (\text{KN}) \quad \text{DBJ13} - 51 \quad (15)$$

Comparative Studies

As shown in Figure 7, the comparison between the first modified formula of the CFST load-carrying capacity to the experimental results shows a clear improvement in the performance of the four codes.

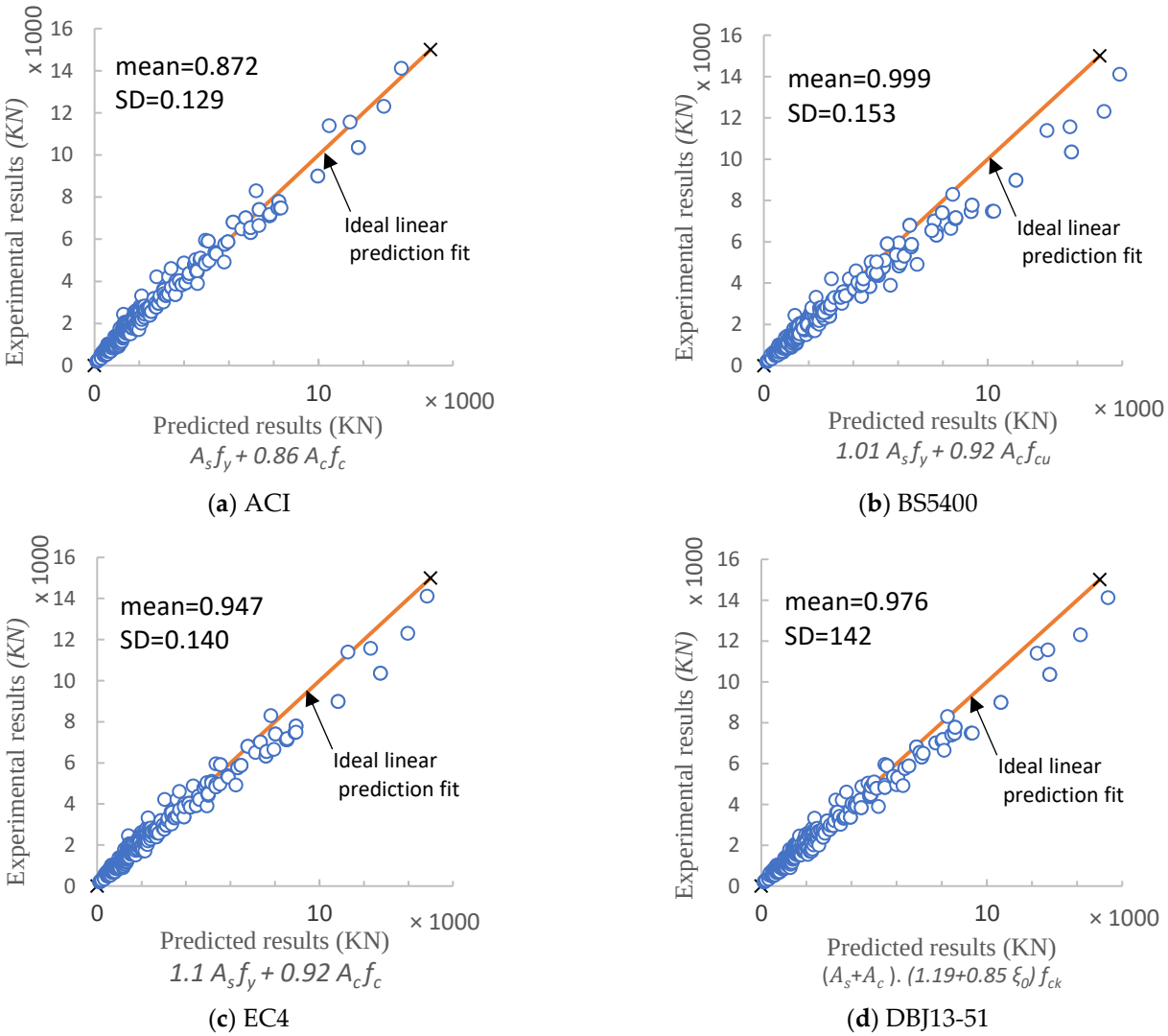


Figure 7. Performance of the first modified approach of the standard formulations.

The most precise mean value (0.999) was achieved using Equation (13) derived from the BS5400 code. In contrast, the less accurate mean was obtained through the modified ACI approach (Equation (12)) and resulted in the same standard deviations of 0.129 as the existing code formulae.

It can be observed in Figure 7 that all approaches provide a better prediction for small section capacities, while the scatter increases as the section capacities increase. Therefore, effort needs to be invested in improving the proposed formulae by considering the magnitude of the sectional capacity. That is, the direction followed in the second proposed formula.

4.2. The Second Proposal to Modify the Existing Design Formulas

In order to improve the scatter of the results for higher section capacities, the second proposed formulation divides the capacity equations into two groups. Similar to the first modification approach, regression analysis was utilized to propose new equations of the four design equations. However, the second modification for the Chinese Standard was divided based on the confinement factor (ξ).

The same VBA code from the first medication proposal was utilized to perform the second proposal after developing it to divide the data into two groups using an iterative method to get the perfectas COV value of all Standards. The load-carrying capacities from the second proposal can be expressed as follows:

ACI

$$N_N\,(u) = \begin{cases} A_S\,f_y + A_C f_C \,\big|< 1800KN & A_S\,f_y + 1.07\,A_C f_C \\ A_S\,f_y + A_C f_C \,\big|\geq 1800KN & A_S\,f_y + 0.9\,A_C f_C \end{cases} \tag{16}$$

BS

$$N_N(u) = \begin{cases} A_S\,f_y + A_C f_U \,\big|< 2000KN & 1.23\;\; A_S\,f_y + 0.8\,A_C f_{CU} \\ A_S\,f_y + A_C f_U \,\big|\geq 2000KN & A_S\,f_y + 0.7\,A_C f_{CU} \end{cases} \tag{17}$$

EC4

$$N_N(u) = \begin{cases} A_S\,f_y + A_C f_C \,\big|< 2000KN & A_S\,f_y + 1.02\,A_C f_C \\ A_S\,f_y + A_C f_C \,\big|\geq 2000KN & A_S\,f_y + 0.78\;\; A_C f_C \end{cases} \tag{18}$$

DJ

$$N_N(u) = \begin{cases} \xi, < 1.250 & (1.2 + 0.85\,\xi) \times F_{CK}\,(KN) \\ \xi, \geq 1.250 & (1.5 + 0.75\,\xi) \times F_{CK}\,(KN) \end{cases} \tag{19}$$

Comparative Studies

Table 1 and Figure 8 illustrate the comparisons between the second proposed equations and the experimental results. Overall, the second proposed formulations give the predictions of mean, standard deviation, and coefficient of variation compared to the existing and first proposed equations. The mean values of the second approach ranged between 0.940 and 0.999, while the standard deviation ranged between 0.129 and 0.142, as shown in Table 1. The scatter of the second proposed equations for the British and Chinese approaches clearly becomes smaller; meanwhile, the mean values of all approaches have significantly improved compared to the experimental results. The improvement in the second modification approach can be obviously observed in Figure 9. The improvement in the predictions of the second modification equations can be attributed to the fact that the existing code equations were proposed for sections with maximum steel and concrete strengths of 450 MPa and 60 MPa, respectively. However, the behavior of higher grades of such materials is relatively different.

Table 1. Comparisons of square and rectangular CFT stub column capacity produced using different equations with the experimental results.

	Mean	SD	COV
ACI	0.867	0.129	0.1488
BS	1.04	0.165	0.1587
EC4	0.938	0.141	0.1503
DJ	0.972	0.142	0.1461
ACI first proposal	0.872	0.129	0.1479
BS5400 first proposal	0.999	0.153	0.1532
EC4 first proposal	0.947	0.14	0.1478
DBJ13-51 first proposal	0.976	0.142	0.1455
ACI second proposal	0.94	0.129	0.1372
BS5400 second proposal	0.999	0.137	0.1371
EC4 second proposal	0.992	0.134	0.1351
DBJ13-51 second proposal	0.991	0.142	0.1433

SD, Standard deviation. COV, coefficient of variation.

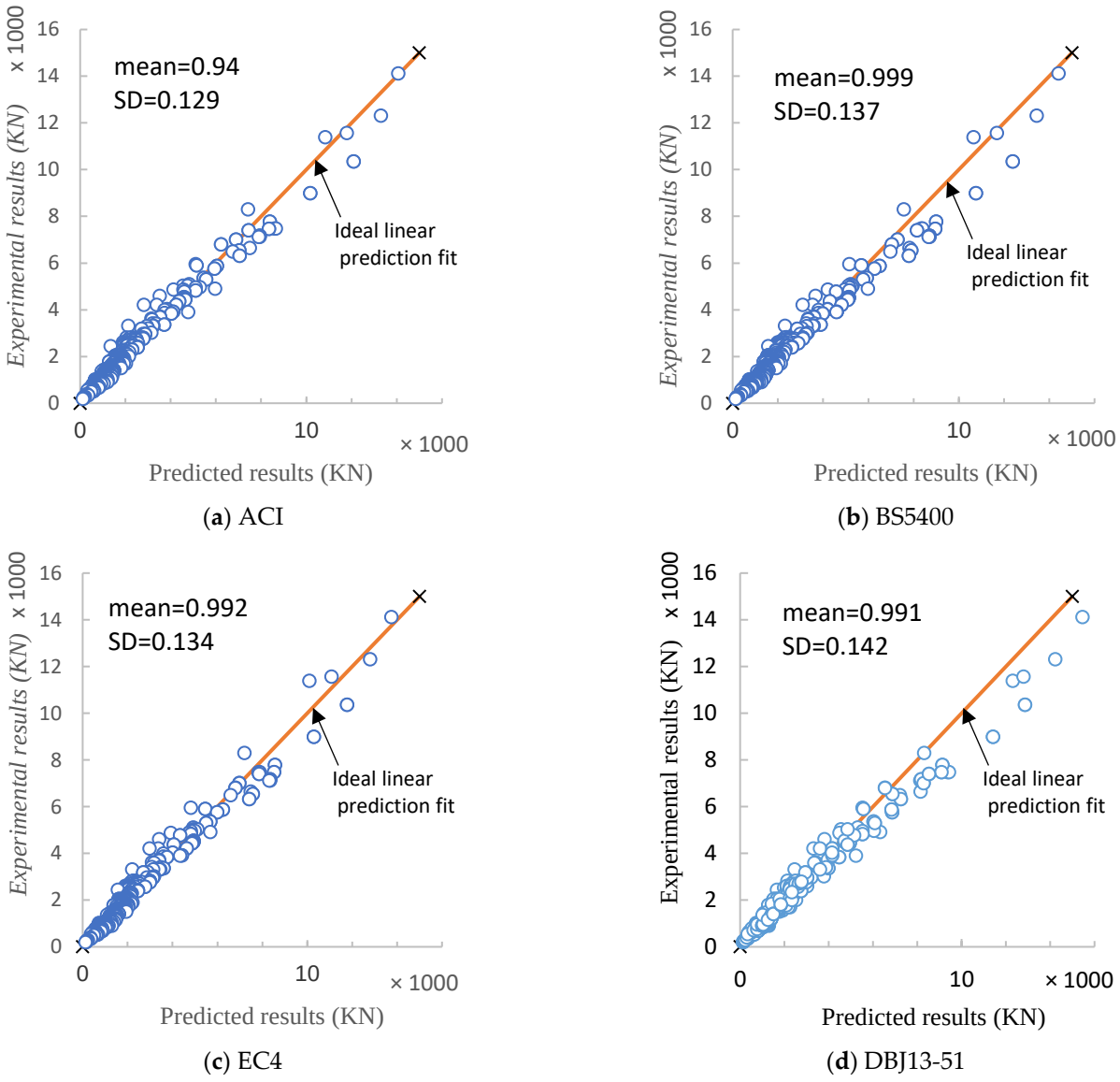


Figure 8. Performance of the second proposal of the standard formulations.

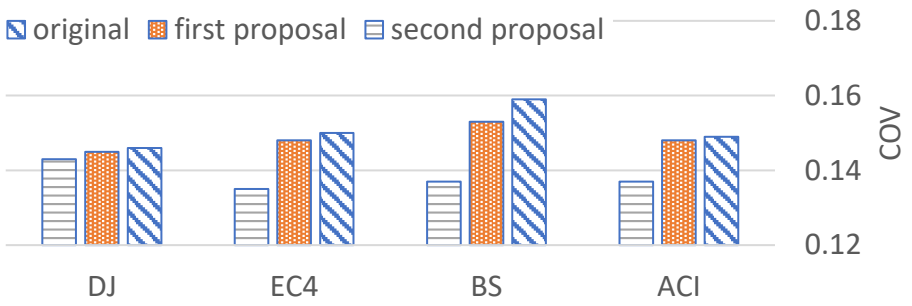


Figure 9. Comparison between the coefficient of variation of the existing and the proposed design approaches.

5. Conclusions

The main objective of this paper is to establish a new comprehensive database consisting of 455 experimental tests of axially loaded square and rectangular concrete-filled steel tubular (CFST) stub columns. The database contains specimens with a concrete core of compressive strengths ranging from normal- to high-strength concrete and steel yield strength ranging from normal to high-strength steel, and with a wide variety of width-to-thickness ratios, steel ratios, and confinement factors. The database was first used to assess the accuracy of four international codes for estimating the axial load capacity and then to suggest more accurate prediction approaches based on the regression analysis method of the collected data. The following conclusions made from this study can be drawn:

1. Despite the considerable number of experimental tests on CFST stub columns, it was found that fewer tests were performed on columns made using high-strength materials. In addition, the tests on large-scale columns were very limited and the majority of these tests were focused on CFST stub columns with small cross-sections.
2. All four codes provided a conservative prediction of CFST stub columns. The Chinese Standard (DBJ13-51) approach gave the most reliable mean value of the predicted load-carrying capacity to experimental results, while the best scatter was achieved by the ACI approach.
3. Better predictions have been generally achieved using the first modified equations of the CFST load-carrying capacity than that of the original four codes. The modified formula based on the BS5400 approach gave the most precise results. However, it was found that the first proposed equations mainly provide accurate predictions for small sectional capacities, while the scattering of the results increases with the increase in section resistance.
4. To improve the scatter of the results, other proposed equations were introduced. It was found that this second proposed approach can provide the most precise results compared to the existing and the first proposed formulas, especially the equation derived from the BS5400 code with a coefficient of variation (COV) of 0.1371.

Author Contributions: F.A.: Conceptualization, Formal analysis, Writing; S.A.O.: Project administration, Supervision, Funding acquisition; A.A.: Conceptualization, Data curation, Formal analysis; M.A.: Data curation, Formal analysis; R.H.: Supervision; F.M.: Supervision. All authors have read and agreed to the published version of the manuscript.

Funding: This research received no external funding.

Data Availability Statement: The resulted data of this study are available on request from the corresponding author.

Conflicts of Interest: The authors declare no conflict of interest.

Appendix A Specimen Database

Table A1. Summary of the collected database.

No	Name of Specimens	b (mm)	h (mm)	t (mm)	f_y (MPa)	f'_c (MPa)	L (mm)	N_u (KN)	Tested by
1	1	142.1	142.1	3.02	255.1	49.2	426.3	1360	
2	2	142.1	142.1	3.02	255.1	49.2	426.3	1400	
3	3	143.1	143.1	3.02	255.1	49.2	429.3	1150	
4	4	101.3	101.3	4.97	347.3	54.2	303.9	1310	
5	5	103.6	103.6	4.9	347.3	54.2	310.8	1340	
6	6	102	102	4.97	347.3	54.2	306	1370	
7	7	142	142	5.11	347.3	54.2	426	2160	
8	8	142	142	5.08	347.3	54.2	426	2250	
9	9	141.4	141.4	5.07	347.3	54.2	424.2	2280	
10	10	141.5	141.5	3.08	255.1	66.2	424.5	1920	
11	11	142.4	142.4	3.05	255.1	66.2	427.2	2060	
12	12	141.6	141.6	3.04	255.1	66.2	424.8	1960	
13	13	103.5	103.5	5.01	347.3	66.2	310.5	1500	
14	14	102.1	102.1	4.97	347.3	66.2	306.3	1330	
15	15	101.9	101.9	5.03	347.3	66.2	305.7	1440	
16	16	142.3	142.3	5.09	347.3	66.2	426.9	2520	Zhang et al., 2005 [16]
17	17	142.4	142.4	5.1	347.3	66.2	427.2	2610	
18	18	139.1	139.1	5.06	347.3	66.2	417.3	1700	
19	20	126.2	161	2.98	255.1	54.2	483	1580	
20	21	126	160.3	2.92	255.1	54.2	480.9	1560	
21	28	101.6	130.3	5.03	347.3	54.2	390.9	1580	
22	29	102.3	130.3	5.14	347.3	54.2	390.9	1600	
23	30	102.3	130.3	5.14	347.3	54.2	390.9	1640	
24	31	136	167.4	5.13	347.3	54.2	502.2	2510	
25	32	135.3	170.8	5.07	347.3	54.2	512.4	2470	
26	35	125.1	160.4	2.85	255.1	66.2	481.2	1855	
27	36	125.6	160	2.88	255.1	66.2	480	2030	
28	37	125	161.1	2.81	255.1	66.2	483.3	2040	
29	41	102.7	125.7	5.15	347.3	66.2	377.1	1840	
30	42	120.4	130	5.03	347.3	66.2	390	1820	
31	43	120.7	132.3	4.98	347.3	66.2	396.9	1725	
32	47	137.1	167.9	5.1	347.3	66.2	503.7	2600	
33	48	133.2	172.7	5.08	347.3	66.2	518.1	2700	
34	120 × 80 × 5	80	120	2.86	386.3	34	200	950	Shakir-Khalil and Zeghiche, 1989 [20]
35	120 × 80 × 5	80	120	5	386.3	30.7	200	900	
36	120 × 80 × 5	80	120	5	384.7	30.7	200	910	
37	120 × 80 × 5	80	120	5	384.7	34	200	900	
38	120 × 80 × 5	80	120	5	343.3	33.2	200	900	
39	120 × 80 × 5	80	120	5	343.3	34.8	200	920	
40	120 × 80 × 5	80	120	5	357.5	34	200	902	
41	120 × 80 × 5	80	120	5	357.5	32	200	900	Shakir-Khalil and Mouli, 1990 [21]
42	120 × 80 × 5	80	120	5	341	32.8	200	920	
43	120 × 80 × 5	80	120	5	341	35.8	200	950	
44	120 × 80 × 5	80	120	5	362.5	32.7	200	955	
45	120 × 80 × 5	80	120	5	362.5	31.4	200	1370	
46	150 × 100 × 5	100	150	5	346.7	35.6	100	1210	
47	150 × 100 × 5	100	150	5	346.7	35.6	200	1340	
48	150 × 100 × 5	100	150	5	346.7	35.8	100	1200	
49	150 × 100 × 5	100	150	5	346.7	35.8	200	1300	
50	150 × 100 × 5	100	150	5	340	36.1	100	1190	
51	150 × 100 × 5	100	150	5	340	36.1	200	1320	
52	150 × 100 × 5	100	150	5	340	36.6	100	1200	

Table A1. *Cont.*

No	Name of Specimens	b (mm)	h (mm)	t (mm)	f_y (MPa)	f'_c (MPa)	L (mm)	N_u (KN)	Tested by
53	CR4-A-2	148	148	4.38	262	25.4	200	1153	
54	CR4-A-4-1	148	148	4.38	262	40.5	200	1414	
55	CR4-A-4-2	148	148	4.38	262	40.5	200	1402	
56	CR4-A-8	148	148	4.38	262	77	200	2108	
57	CR4-C-2	215	215	4.38	262	25.4	200	1777	
58	CR4-C-4-1	215	215	4.38	262	41.1	200	2424	
59	CR4-C-4-2	215	215	4.38	262	41.1	200	2393	
60	CR4-C-8	215	215	4.38	262	80.3	200	3837	
61	CR4-D-2	323	323	4.38	262	25.4	200	3367	
62	CR4-D-4-1	323	323	4.38	262	41.1	200	4950	
63	CR4-D-4-2	323	323	4.38	262	41.1	200	4830	
64	CR4-D-8	324	324	4.38	262	80.3	200	7481	
65	CR6-A-2	144	144	6.36	618	25.4	200	2572	
66	CR6-A-4-1	144	144	6.36	618	40.5	200	2808	
67	CR6-A-4-2	144	144	6.36	618	40.5	200	2765	
68	CR6-A-8	144	144	6.36	618	77	200	3399	
69	CR6-C-2	211	211	6.36	618	25.4	200	3920	
70	CR6-C-4-1	211	211	6.36	618	40.5	200	4428	
71	CR6-C-4-2	211	211	6.36	618	40.5	200	4484	
72	CR6-C-8	211	211	6.36	618	77	200	5758	
73	CR6-D-2	319	319	6.36	618	25.4	200	6320	
74	CR6-D-4-1	319	319	6.36	618	41.1	200	7780	
75	CR6-D-4-2	318	318	6.36	618	41.1	200	7473	
76	CR6-D-8	319	319	6.36	618	85.1	200	10357	Sakino,
77	CR8-A-2	120	120	6.47	835	25.4	200	2819	2004 [18]
78	CR8-A-4-1	120	120	6.47	835	40.5	200	2957	
79	CR8-A-4-2	120	120	6.47	835	40.5	200	2961	
80	CR8-A-8	119	119	6.47	835	77	200	3318	
81	CR8-C-2	175	175	6.47	835	25.4	200	4210	
82	CR8-C-4-1	175	175	6.47	835	40.5	200	4493	
83	CR8-C-4-2	175	175	6.47	835	40.5	200	4542	
84	CR8-C-8	175	175	6.47	835	77	200	5366	
85	CR8-D-2	265	265	6.47	835	25.4	200	6546	
86	CR8-D-4-1	264	264	6.47	835	41.1	200	7117	
87	CR8-D-4-2	265	265	6.47	835	41.1	200	7172	
88	CR8-D-8	265	265	6.47	835	80.3	200	8990	
89	CR4-A-4-3	210	210	5.48	294	39.1	200	3183	
90	CR4-A-9	211	211	5.48	294	91.1	200	4773	
91	CR4-C-4-3	210	210	4.5	277	39.1	200	2713	
92	CR4-C-9	211	211	4.5	277	91.1	200	4371	
93	CR6-A-4-3	211	211	8.83	536	39.1	200	5898	
94	CR6-A-9	211	211	8.83	536	91.1	200	7008	
95	CR6-C-4-3	204	204	5.95	540	39.1	200	4026	
96	CR6-C-9	204	204	5.95	540	91.1	200	5303	
97	CR8-A-4-3	180	180	9.45	825	39.1	200	6803	
98	CR8-A-9	180	180	9.45	825	91.1	200	7402	
99	CR8-C-4-3	180	180	6.6	824	39.1	200	5028	
100	CR8-C-9	180	180	6.6	824	91.1	200	5873	
101	1	160	160	3.46	363	64.8	200	2011	
102	2	160	160	3.46	363	64.8	200	2333	
103	3	160	160	3.46	363	44.4	200	1784	Wang,
104	4	160	160	3.46	363	44.4	200	1812	2014 [19]
105	5	160	160	5.43	353	64.8	200	2751	
106	6	160	160	5.43	353	64.8	200	2791	

Table A1. *Cont.*

No	Name of Specimens	b (mm)	h (mm)	t (mm)	f_y (MPa)	f'_c (MPa)	L (mm)	N_u (KN)	Tested by
107	DF3	114.3	114.3	9.63	258	32.6	406	2442	Neogi and Chapman, 1969 [34]
108	DF4	114.9	114.9	4.39	258	32.6	406	897	
109	scdz1-2	120	120	3.84	330.1	16.7	360	882	Wei and Han, 2000 [35]
110	scdz1-3	120	120	3.84	330.1	16.7	360	921.2	
111	scdz1-4	120	120	3.84	330.1	26.4	360	1080	
112	scdz1-5	120	120	3.84	330.1	28.2	360	1078	
113	scdz2-3	140	140	3.84	330.1	29.3	420	1499.4	
114	scdz2-4	140	140	3.84	330.1	29.3	420	1470	
115	scdz3-1	120	120	5.86	321.1	16.1	360	1176	
116	scdz3-2	120	120	5.86	321.1	16.1	360	1117.2	
117	scdz3-4	120	120	5.86	321.1	28.2	360	1460.2	
118	scdz3-5	120	120	5.86	321.1	28.2	360	1372	
119	scdz4-3	140	140	5.86	321.1	29.3	420	2009	
120	scdz4-4	140	140	5.86	321.1	29.3	420	1906.1	
121	2fp3-1	100	100	2	284.6	32.4	400	588	Zhang and Zhou, 2000 [36]
122	2fp3-6	100	100	2	284.6	32.4	400	656.6	
123	2fp3-22	100	100	2	284.6	32.4	400	745	
124	2fp4-10	100	100	2	284.6	32.4	400	705.6	
125	2fp4-14	100	100	2	284.6	32.4	400	666.4	
126	2fp4-16	100	100	2	284.6	32.4	400	696	
127	2fp4-23	100	100	2	284.6	32.4	400	725	
128	2fp4-24	100	100	2	284.6	32.4	400	745	
129	3fp3-25	100	100	3	288.2	32.4	400	852	
130	3fp3-36	100	100	3	288.2	32.4	400	892	
131	3fp3-8	100	100	3	288.2	32.4	400	882	
132	3fp3-26	100	100	3	288.2	32.4	400	931	
133	3fp3-5	100	100	3	288.2	32.4	400	882	
134	3fp4-11	100	100	3	288.2	32.4	400	891	
135	3fp4-17	100	100	3	288.2	32.4	400	833	
136	3fp4-20	100	100	3	288.2	32.4	400	872	
137	5fp3-4	100	100	5	403.4	32.4	400	1195	
138	5fp3-27	100	100	5	403.4	32.4	400	1068	
139	5fp3-28	100	100	5	403.4	32.4	400	1294	
140	5fp3-35	100	100	5	403.4	32.4	400	1274	
141	5fp3-29	100	100	5	403.4	32.4	400	1313	
142	5fp4-13	100	100	5	403.4	32.4	400	1294	
143	5fp4-18	100	100	5	403.4	32.4	400	1244.6	
144	5fp4-21	100	100	5	403.4	32.4	400	1323	
145	5fp4-30	100	100	5	403.4	32.4	400	1313	
146	5fp4-31	100	100	5	403.4	32.4	400	1274	
147	5fp4-32	100	100	5	403.4	32.4	400	1244.6	
148	4fp3-7	100	100	4	239.8	32.4	400	1019	
149	4fp3-9	100	100	4	239.8	32.4	400	980	
150	4fp3-2	100	100	4	239.8	32.4	400	882	
151	4fp3-33	100	100	4	239.8	32.4	400	901.6	
152	4fp3-34	100	100	4	239.8	32.4	400	980	
153	4fp4-15	100	100	4	239.8	32.4	400	1000	
154	4fp4-19	100	100	4	239.8	32.4	400	970	
155	4fp4-35	100	100	4	239.8	32.4	400	921.2	
156	4fp4-36	100	100	4	239.8	32.4	400	960.4	

Table A1. *Cont.*

No	Name of Specimens	b (mm)	h (mm)	t (mm)	f_y (MPa)	f'_c (MPa)	L (mm)	N_u (KN)	Tested by
157	1A	100	100	2.29	194.2	32	300	497.4	Tomii and Sakino, 1979 [37]
158	1B	100	100	2.29	194.2	32	300	498	
159	2A	100	100	2.2	339.4	21.4	300	511	
160	2B	100	100	2.2	339.4	21.4	300	510	
161	4A	100	100	2.99	288.4	20.6	300	529	
162	3B	100	100	2.99	288.4	20.6	300	528	
163	4A	100	100	4.25	284.5	19.8	300	667	
164	4B	100	100	4.25	284.5	19.8	300	666	
165	27	250	250	8	379	33	500	4870	Grauers M, 1993 [38]
166	28	250	250	8	379	91	500	8300	
167	CR4A2	148	148	4.38	262	25.4	444	1153	Inai and Sakino, 1996 [39]
168	CR4A4.1	148	148	4.38	262	40.5	444	1414	
169	CR4A4.2	148	148	4.38	262	40.5	444	1402	
170	CR4A8	148	148	4.38	262	77	444	2108	
171	CR4C2	215	215	4.38	262	25.4	645	1777	
172	CR4C4.1	215	215	4.38	262	41.1	645	2424	
173	CR4C4.2	215	215	4.38	262	41.1	645	2393	
174	CR4C8	215	215	4.38	262	80.3	645	3837	
175	CR4D2	323	323	4.38	262	25.4	969	3367	
176	CR4D4.1	323	323	4.38	262	41.1	969	5950	
177	CR4D4.2	323	323	4.38	262	41.1	969	4830	
178	CR4D8	323	323	4.38	262	80.3	969	7481	
179	CR6A2	144	144	6.36	618	25.4	432	2572	
180	CR6A4.1	144	144	6.36	618	40.5	432	2808	
181	CR6A4.2	144	144	6.36	618	40.5	432	2765	
182	CR6A8	144	144	6.36	618	77	432	3399	
183	CR6C2	211	211	6.36	618	25.4	633	3920	
184	CR6C4.1	211	211	6.36	618	40.5	633	4428	
185	CR6C4.2	211	211	6.36	618	40.5	633	4484	
186	CR6C8	211	211	6.36	618	77	633	5758	
187	CR6D2	319	319	6.36	618	25.4	957	6320	
188	CR6D4.1	319	319	6.36	618	41.1	957	7780	
189	CR6D4.2	318	318	6.36	618	41.1	954	7473	
190	CR6D8	319	319	6.36	618	85.1	957	10357	
191	CR8A2	120	120	6.36	618	25.4	360	2819	
192	CR8A4.1	120	120	6.47	835	40.5	360	2957	
193	CR8A4.2	120	120	6.47	835	40.5	360	2961	
194	CR8A8	120	120	6.47	835	77	360	3318	
195	CR8C2	175	175	6.47	835	25.4	525	4210	
196	CR8C4.1	175	175	6.47	835	40.5	525	4493	
197	CR8C4.2	175	175	6.47	835	40.5	525	4542	
198	CR8C8	175	175	6.47	835	77	525	5366	
199	CR8D2	265	265	6.47	835	25.4	795	6546	
200	CR8D4.1	265	265	6.47	835	41.1	795	7117	
201	CR8D4.2	265	265	6.47	835	41.1	795	7172	
202	CR8D8	265	265	6.47	835	80.3	795	8990	
203	CR4A4.3	210	210	5.48	294	39.1	630	3184	
204	CR4A9	211	211	5.48	294	91.1	633	4775	
205	CR4C4.3	210	210	4.5	277	39.1	630	2714	
206	CR4C9	211	211	4.5	277	91.1	633	4372	
207	CR6A4.3	211	211	8.83	536	39.1	633	5900	
208	CR6A9	211	211	8.83	536	91.1	633	7010	
209	CR6C4.3	204	204	5.95	540	39.1	612	4027	
210	CR6C9	204	204	5.95	540	91.1	612	5305	
211	CR8A4.3	180	180	9.45	825	39.1	540	6805	
212	CR8A9	180	180	9.45	825	91.1	540	7405	

Table A1. *Cont.*

No	Name of Specimens	b (mm)	h (mm)	t (mm)	f_y (MPa)	f'_c (MPa)	L (mm)	N_u (KN)	Tested by
213	CR8C4.3	180	180	6.6	824	31.1	540	5030	
214	CR8C9	180	180	6.6	824	91.1	540	5875	
215	CR8-6-10	200	200	6.16	781	119	600	6645	Nakahara and Sakino, 1998 [40]
216	CR8-3-10	200	200	3.17	781	119	600	4910	
217	CR4-6-10	200	200	6.39	310	119	600	4965	
218	CR4-3-10	200	200	3.09	310	119	600	3899	
219	SC-32-80	305	305	8.9	560	110	1220	14116	Varma, 2000 [41]
220	SC-48080	305	305	6.1	660	110	1220	12307	
221	Sc-32-46	305	305	8.6	259	110	1220	11390	
222	SC-48-46	305	305	5.8	471	110	1220	11568	
223	1	152.4	152.4	4.43	389	46.2	300	1906	Lu and Kennedy, 1992 [42]
224	2	152.4	152.4	8.95	432	45.4	300	3307	
225	3	152	153.4	6.17	377	43.6	300	3317	
226	4	152.2	153	9.04	394	47.2	300	4208	
227	S10D-2A	100.2	100.2	2.18	300	25.7	300	609	Yamamoto et al., 2000 [43]
228	S20D-2A	200.3	200.3	4.35	323	29.6	601	2230	
229	S30D-2A	300.5	300.5	6.1	395	26.5	902	5102	
230	S10D-4A	100.1	100.1	2.18	300	53.7	300	851	
231	S20D-4A	200.1	200.1	4.35	323	57.9	601	3201	
232	S30D-4A	300.7	300.7	6.1	395	52.2	902	6494	
233	S10D-6A	100.1	100.1	2.18	300	61	300	911	
234	S20D-6A	200.3	200.3	4.35	323	63.7	601	3417	
235	1 rc1-1	100	100	2.86	228	47.44	300	760	Han and Yao, 2002 [44]
236	2 rc1-2	100	100	2.86	228	47.44	300	800	
237	3 rc2-1	120	120	2.86	228	47.44	360	992	
238	4 rc2-2	120	120	2.86	228	47.44	360	1050	
239	5 rc3-1	100	110	2.86	228	47.44	330	844	
240	6 rc3-2	100	110	2.86	228	47.44	330	860	
241	7 rc4-1	135	150	2.86	228	47.44	450	1420	
242	8 rc4-2	135	150	2.86	228	47.44	450	1340	
243	9 rc5-1	70	90	2.86	228	47.44	270	554	
244	10 rc5-2	70	90	2.86	228	47.44	270	576	
245	11 rc6-1	75	100	2.86	228	47.44	300	640	
246	12 rc6-2	75	100	2.86	228	47.44	300	672	
247	13 rc7-1	90	120	2.86	228	47.44	360	800	
248	14 rc7-2	90	120	2.86	228	47.44	360	760	
249	15 rc8-1	105	140	2.86	228	47.44	420	1044	
250	16 rc8-2	105	140	2.86	228	47.44	420	1086	
251	17 rc9-1	115	150	2.86	228	47.44	450	1251	
252	18 rc9-2	115	150	2.86	228	47.44	450	1218	
253	19 rc10-1	120	160	7.6	194	47.44	480	1820	
254	20 rc10-2	120	160	7.6	194	47.44	480	1770	
255	S3	100.7	100.7	9.6	400	24.64	301	1550	Lam and Williams, 2004 [45]
256	S4	101	101	9.6	400	74.88	300	2000	
257	S5	99.9	99.9	4.9	289	24.64	301	800	
258	S6	99.8	99.8	4.9	300	74.88	300	900	
259	S7	100.1	100.1	4.2	333	27.76	301	700	
260	S8	100	100	4.2	333	27.76	302	680	
261	S9	100	100	4.1	333	77.76	299	1130	
262	S10-g	100	100	4.1	333	77.76	300	970	
263	S12	100	100	4.1	333	46.08	301	880	
264	S13-g	99.9	99.9	4	333	46.08	301	830	
265	S14	101	101	9.6	400	46.08	302	1800	
266	S15-g	99.8	99.8	4.8	289	25.52	302	780	

Table A1. *Cont.*

No	Name of Specimens	b (mm)	h (mm)	t (mm)	f_y (MPa)	f'_c (MPa)	L (mm)	N_u (KN)	Tested by
267	S16	99.7	99.7	4.7	289	46.56	301	1000	
268	S17-g	99.7	99.7	4.73	289	79.12	302	1050	
269	S18	99.9	99.9	4.1	333	79.12	301	1130	
270	sssc-1	200	200	3	303.5	46.8	600	2458	Han and Yao, 2004 [46]
271	sssc-2	200	200	3	303.5	46.8	601	2594	
272	ssh-1	200	200	3	303.5	46.8	602	2306	
273	ssh-2	200	200	3	303.5	46.8	603	2284	
274	ssv-1	200	200	3	303.5	46.8	604	2550	
275	ssv-2	200	200	3	303.5	46.8	605	2587	
276	1	199	199	1.8	192.4	27.7	796	1403	Zhang Z-G, 1984 [47]
277	2	197	197	1.55	192.4	27.7	797	1413	
278	3	199	199	1.5	192.4	27.7	798	1362	
279	4	199	199	1.63	192.4	25.4	798	1163	
280	5	198	198	1.66	192.4	25.6	794	1310	
281	6	199	199	1.68	192.4	25.6	796	1110	
282	7	199	199	1.91	246.7	27.6	792	1360	
283	8	199	199	1.86	246.7	27.6	797	1417	
284	9	199	199	1.62	246.7	27.6	798	1360	
285	10	198	198	1.72	246.7	25.7	797	1210	
286	11	199	199	1.69	246.7	25.7	797	1160	
287	12	199	199	1.66	246.7	25.8	796	1065	
288	13	150	150	1.52	246.7	37.1	595	905	
289	14	149	149	1.47	246.7	37.4	596	1000	
290	15	150	150	1.6	246.7	37.4	598	950	
291	16	148	148	1.57	246.7	25.8	598	660	
292	17	149	149	1.64	246.7	25.9	595	710	
293	18	200	200	2.93	256.4	27.6	793	1764	
294	19	201	201	2.92	256.4	27.6	796	1760	
295	20	198	198	2.92	256.4	27.6	797	1760	
296	21	199	199	2.91	256.4	25.8	793	1546	
297	22	200	200	2.93	256.4	25.9	792	1560	
298	23	200	200	3.93	256.4	25.9	794	1509	
299	24	199	199	3.99	279	36.2	796	2100	
300	25	200	200	3.96	279	36.4	796	2100	
301	26	200	200	4.93	294	36	796	2439	
302	27	200	200	4.92	294	36	796	2465	
303	28	149	149	3.91	279	37	598	1300	
304	29	149	149	3.96	279	37	598	1340	
305	30	149	149	3.94	279	37	597	1350	
306	31	198	198	5.66	234.7	35.9	796	2330	
307	32	198	198	5.96	234.7	36	797	2800	
308	33	198	198	5.69	234.7	36.5	796	2190	
309	34	150	150	4.93	294.9	36.9	595	1645	
310	35	150	150	4.95	294.9	36.9	594	1630	
311	36	150	150	4.96	294.9	36.9	595	1650	
312	37	199	199	7.83	238.3	35.7	797	2700	
313	38	200	200	7.8	238.3	35.7	796	2590	
314	39	99	99	4.9	294.9	37.1	398	960	
315	40	99	99	4.92	294.9	37.4	397	980	
316	41	99	99	4.86	294.9	37.9	399	900	
317	42	149	149	7.67	238.3	36.6	596	1845	
318	43	149	149	7.67	238.3	36.6	596	1850	
319	44	149	149	7.58	238.3	36.6	598	1750	
320	45	98	98	5.74	234.7	37.9	399	950	
321	46	99	99	5.84	234.7	37.9	398	950	
322	47	99	99	5.85	234.7	38	395	850	
323	48	99	99	7.72	238.3	38	396	1100	

Table A1. *Cont.*

No	Name of Specimens	b (mm)	h (mm)	t (mm)	f_y (MPa)	f'_c (MPa)	L (mm)	N_u (KN)	Tested by
324	49	100	100	7.78	238.3	38	398	1050	
325	50	99	99	7.82	238.3	38	397	1000	
326	1	200	200	5	227	24	600	2061	
327	2	200	200	5	227	28.8	600	2530	
328	3	200	200	5	227	36.8	600	2468	Lu et al., 1999 [48]
329	4	300	300	5	227	24	900	3621	
330	5	300	300	5	227	28.8	900	4603	
331	6	300	300	5	227	36.8	900	4872	
332	S-80-F-1	80.2	80.2	1.6	279.9	32.9	240	353	
333	S-80-F-2	80.9	80.9	1.6	279.9	32.9	240	347	
334	S-110-F-1	110	110	1.5	279.9	32.9	330	510	Guo Lanhui, 2006 [49]
335	S-110-F-2	109.8	109.8	1.5	279.9	32.9	330	522	
336	S-150-F-1	149.3	149.3	3.6	279.9	41.8	450	1771	
337	S-150-F-2	149.3	149.3	3.6	279.9	41.8	450	1785	
338	A1	120	120	5.8	300	74.7	360	1697	
339	A2	120	120	5.8	300	92	360	1919	
340	1A3-1	200	200	5.8	300	74.7	600	3996	
341	1A3-2	200	200	5.8	300	74.7	600	3862	
342	1A4-1	100	130	5.8	300	74.7	390	1601	
343	1A4-2	100	130	5.8	300	74.7	390	1566	
344	1A5-1	100	130	5.8	300	92	390	1854	Liu and Gho, 2005 [50]
345	1A5-2	100	130	5.8	300	92	390	1779	
346	1A6-1	170	220	5.8	300	74.7	660	3684	
347	1A6-2	170	220	5.8	300	74.7	660	3717	
348	1A9-1	120	120	4	495	56	360	1739	
349	1A9-2	120	120	4	495	56	360	1718	
350	1A12-1	130	130	4	495	56	390	1963	
351	1A12-2	130	130	4	495	56	390	1988	
352	C1-1	98.2	100.3	4.18	550	56.6	300	1490	
353	C1-2	100.6	101.5	4.18	550	56.6	300	1535	
354	C2-1	101.1	101.2	4.18	550	65.7	300	1740	Liu et al., 2003 [51]
355	C2-2	100.4	100.7	4.18	550	65.7	300	1775	
356	C3	181.2	182.8	4.18	550	56.6	540	3590	
357	C4	180.4	181.8	4.18	550	65.7	540	4210	
358	R1-1	120	120	4	495	58.4	360	1701	
359	R1-2	120	120	4	495	58.4	360	1657	
360	R4-1	130	130	4	495	58.4	390	2020	
361	R4-2	130	130	4	495	58.4	390	2018	
362	R7-1	108	108	4	495	77.6	320	1749	Liu, 2005 [52]
363	R7-2	108	108	4	495	77.6	320	1824	
364	R10-1	140	140	4	495	77.6	420	2752	
365	R10-2	140	140	4	495	77.6	420	2828	
366	R11-1	125	160	4	495	77.6	480	2580	
367	R11-2	125	160	4	495	77.6	480	2674	
368	43	101.3	101.3	4.97	347.3	49.4	300	1310	
369	45	103.6	103.6	4.9	347.3	49.4	300	1340	
370	46	102	102	4.97	347.3	49.4	300	1370	
371	23	142	142	5.11	347.3	49.4	420	2160	
372	27	142	142	5.08	347.3	49.4	420	2250	Ye Zaili, 2001 [53]
373	29	141.4	141.4	5.07	347.3	49.4	420	2280	
374	96	142.1	142.1	3.02	255.1	44.9	420	1360	
375	97	142.1	142.1	3.02	255.1	44.9	420	1400	
376	69	142.1	142.1	2.01	305.1	44.9	420	1328	
377	70	142.1	142.1	2.01	305.1	44.9	420	1364	

Table A1. *Cont.*

No	Name of Specimens	b (mm)	h (mm)	t (mm)	f_y (MPa)	f'_c (MPa)	L (mm)	N_u (KN)	Tested by
378	71	140.9	140.9	2.02	305.1	44.9	420	1280	
379	105	103.5	103.5	5.01	347.3	58.6	300	1500	
380	106	102.1	102.1	4.97	347.3	58.6	300	1330	
381	113	101.9	101.9	5.03	347.3	58.6	300	1440	
382	161	142.3	142.3	5.09	347.3	58.6	420	2520	
383	162	142.4	142.4	5.1	347.3	58.6	420	2610	
384	130	143.2	143.2	2.03	305.1	58.6	420	1990	
385	133	142.3	142.3	2.01	305.1	58.6	420	1855	
386	156	140.5	140.5	2	305.1	58.6	420	1780	
387	127	141.5	141.5	3.08	255.1	58.6	420	1920	
388	134	142.4	142.4	3.05	255.1	58.6	420	2060	
389	129	141.6	141.6	3.04	255.1	58.6	420	1960	
390	159	149.1	149.1	5.06	347.3	58.6	420	1700	
391	93	143.1	143.1	3.02	255.1	44.9	420	1150	
392	22	101.6	130.3	5.03	347.3	49.4	390	1580	
393	38	102.3	130.3	5.14	347.3	49.4	390	1600	
394	39	102.3	130.3	5.14	347.3	49.4	390	1640	
395	85	120.2	166.3	2.94	255.1	49.4	480	1580	
396	86	126.2	161	2.98	255.1	49.4	480	1580	
397	88	126	160.3	2.92	255.1	49.4	480	1560	
398	4	136.1	167.4	5.13	347.3	49.4	480	2510	
399	5	135.3	170.8	5.07	347.3	49.4	510	2470	
400	136	102.7	125.7	5.15	347.3	58.6	390	1840	
401	150	120.4	130	5.03	347.3	58.6	390	1820	
402	151	102.7	132.3	4.98	347.3	58.6	390	1725	
403	160	122.5	157.1	2.01	305.1	58.6	480	1800	
404	163	119	161.9	2	305.1	58.6	480	1740	
405	135	125.1	160.4	2.85	255.1	58.6	480	1855	
406	137	125.6	160	2.88	255.1	58.6	480	2030	
407	152	125	161.1	2.81	255.1	58.6	480	2040	
408	153	137.1	167.9	5.1	347.3	58.6	480	2600	
409	154	133.2	172.7	5.08	347.3	58.6	480	2700	
410	60	122.7	160.2	2.03	305.1	49.4	480	1400	
411	62	119.4	160.1	2.01	305.1	49.4	480	1420	
412	65	124.3	161.5	2	305.1	49.4	480	1320	
413	S-150-F-1	149.3	149.3	3.63	283.6	31.7	448	1771	Guo et al., 2006 [54]
414	S-150-F-2	149.3	149.3	3.63	283.6	31.7	448	1785	
415	S-150-CF-1 o	149.1	149.1	3.69	283.6	31.7	448	1409	
416	S-150-CF-2 o	149	149	3.59	283.6	31.7	448	1370	
417	S-150-C-1 c	148.6	148.6	3.67	283.6	31.7	448	1433	
418	S-150-C-2 c	149.4	149.4	3.64	283.6	31.7	448	1399	
419	S-120-P2 s	120	120	2.65	340	21.9	360	778	

References

1. Zhao, X.-L.; Han, L.-H.; Lu, H. *Concrete-Filled Tubular Members and Connections*; Spon Press: London, UK, 2010.
2. Abdalla, S.H. *Behavior of Concrete Filled Steel Tube (CFST) Under Different Loading Conditions*; American University of Sharjah: Sharjah, United Arab Emirates, 2012.
3. Wang, Z.; Liu, Z.; Zhou, X. Experimental Investigation of Special-Shaped Concrete-Filled Square Steel Tube Composite Columns with Steel Hoops under Axial Loads. *Materials* **2022**, *15*, 4179. [CrossRef] [PubMed]
4. Alatshan, F.; Osman, S.A.; Hamid, R.; Mashiri, F. Stiffened concrete-filled steel tubes: A systematic review. *Thin-Walled Struct.* **2020**, *148*, 106590. [CrossRef]
5. Chang, Z.H.; Azmi, M.R.; Yatim, M.Y.M. Behaviour of Concrete-Filled Double Skin Tubular Short Column with Plate Stiffeners Welded Intermittently under Axial Compression. *Buildings* **2022**, *12*, 567. [CrossRef]
6. Rahnavard, R.; Craveiro, H.D.; Lopes, M.; Simões, R.A.; Laím, L.; Rebelo, C. Concrete-filled cold-formed steel (CF-CFS) built-up columns under compression: Test and design. *Thin-Walled Struct.* **2022**, *179*, 109603. [CrossRef]

7. Rahnavard, R.; Craveiro, H.D.; Simões, R.A.; Laím, L.; Santiago, A. Buckling resistance of concrete-filled cold-formed steel (CF-CFS) built-up short columns under compression. *Thin-Walled Struct.* **2022**, *170*, 108638. [CrossRef]
8. Luo, Y.; Zhao, Y.; Chen, Y.; Lin, X.; Yan, J. Experimental Studies on Seismic Performance of UHPSFRC-Filled Square Steel Tubular Columns. *Buildings* **2022**, *12*, 798. [CrossRef]
9. Dabbagh, N.M.R.; Wan Badaruzzaman, W.H.; Al Zand, A.W.; Kazemzadeh Azad, S.; Uy, B.; Azmi, M.R.; Alatshan, F. A systematic review on CFST members under impulsive loading. *Thin-Walled Struct.* **2022**, *179*, 109503. [CrossRef]
10. Xu, B.; Wang, L.; Xiang, C.; Han, Z. Analysis of Buckling Deformation for the Side Plate of Rectangular CSFT Column Based on Plate Theory with Bi-Axial Loads. *Buildings* **2022**, *12*, 626. [CrossRef]
11. Alatshan, F.; Osman, S.A.; Mashiri, F.; Hamid, R. Explicit Simulation of Circular CFST Stub Columns with External Steel Confinement under Axial Compression. *Materials* **2020**, *13*, 23. [CrossRef]
12. Han, L.-H.; Li, W.; Bjorhovde, R. Developments and advanced applications of concrete-filled steel tubular (CFST) structures: Members. *J. Constr. Steel Res.* **2014**, *100*, 211–228. [CrossRef]
13. Goode, C.D. ASCCS Database of Concrete-Filled Steel Tube Columns. Available online: https://www.bradford.ac.uk/sustainable-environments/asccs/columns-database/ (accessed on 21 December 2022).
14. Lam, D.; Gardner, L. Structural design of stainless steel concrete filled columns. *J. Constr. Steel Res.* **2008**, *64*, 1275–1282. [CrossRef]
15. Ellobody, E.; Young, B. Design and behaviour of concrete-filled cold-formed stainless steel tube columns. *Eng. Struct.* **2006**, *28*, 716–728. [CrossRef]
16. Zhang, S.; Guo, L.; Ye, Z.; Wang, Y. Behavior of Steel Tube and Confined High Strength Concrete for Concrete-Filled RHS Tubes. *Adv. Struct. Eng.* **2005**, *8*, 101–116. [CrossRef]
17. Uy, B.; Tao, Z.; Han, L.-H. Behaviour of short and slender concrete-filled stainless steel tubular columns. *J. Constr. Steel Res.* **2011**, *67*, 360–378. [CrossRef]
18. Sakino, K.; Nakahara, H.; Morino, S.; Nishiyama, I. Behavior of Centrally Loaded Concrete-Filled Steel-Tube Short Columns. *J. Struct. Eng.* **2004**, *130*, 180–188. [CrossRef]
19. Wang, W.-H.; Han, L.-H.; Li, W.; Jia, Y.-H. Behavior of concrete-filled steel tubular stub columns and beams using dune sand as part of fine aggregate. *Constr. Build. Mater.* **2014**, *51*, 352–363. [CrossRef]
20. Shakir-Khalil, H.; Zeghiche, J. Experimental behaviour of concrete-filled rolled rectangular hollow-section columns. *Struct. Eng.* **1989**, *67*, 346–353.
21. Shakir-Khalil, H.; Mouli, M. Further tests on concrete-filled rectangular hollow-section columns. *Struct. Eng.* **1990**, *68*, 405–413.
22. *EN 1994-2: Eurocode 4*; Design of Composite Steel and Concrete Structures-Part 2: General Rules and Rules for Bridges. European Committee for Standardisation: Brussels, Belgium, 1994.
23. *EC:2. 1-1*; Eurocode 2: Design of Concrete Structures: Part 1-1: General Rules and Rules for Buildings. British Standards Institution: London, UK, 2004.
24. *ACI:318*; Building Code Requirements for Reinforced Concrete and Commentary. American Concrete Institute International: Farmington Hills, MI, USA, 2011.
25. *Architectural Institute of Japan (AIJ)*; Standards for Structural Calculation of Steel Reinforced Concrete Structures. Architectural Institute of Japan: Tokyo, Japan, 2001.
26. *AS AS5100*; 2-2004, Bridge Design—Part 2: Design Loads. Standards Australia: Sydney, Australia, 2004.
27. *BSI BS5400*; Steel, Concrete and Composite Bridges, Part 5, Code of Practice for the Design of Composite Bridges. British Standard Institution: London, UK, 2005.
28. *DBJ:13-51*; Technical Specification for Concrete-filled Steel Tubular Structures. The Construction Department of Fujian Province: Fuzhou, China, 2003.
29. *3678, A.N.*; Structural Steel—Hot-Rolled Plates, Floorplates and Slabs. Australian/New Zealand Standard. Standards Australia: Sydney, Australia, 1996.
30. *EN:10025*; Hot Rolled Products of Structural Steels, Part 6: Technical Delivery Conditions for Flat Products of High Yield Strength Structural Steels in the Quenched and Tempered Condition. The European Standard EN: Brussels, Belgium, 2004.
31. *GB:50017*; Code for Design of Steel Structures. National Standard of P. R. China: Beijing, China, 2003.
32. Lu, Z.-H.; Zhao, Y.-G. Suggested empirical models for the axial capacity of circular CFT stub columns. *J. Constr. Steel Res.* **2010**, *66*, 850–862. [CrossRef]
33. Hanoon, A.N.; Al Zand, A.W..; Yaseen, Z.M. Designing new hybrid artificial intelligence model for CFST beam flexural performance prediction. *Eng. Comput.* **2022**, *38*, 3109–3135. [CrossRef]
34. Neogi, P.; Sen, H.; Chapman, J. Concrete-filled tubular steel columns under eccentric loading. *Struct. Eng.* **1969**, *47*, 187–195.
35. Zhuobin, W.; Linhai, H. RESEARCH ON THE BEARING CAPACITY OF EARLY-STRENGTH CONCRETE FILLED SQUARE STEEL TUBE. In *Proceedings of Composite and Hybrid Structures: Proceedings of the Sixth ASCCS International Conference on Steel-Concrete Composite Structures, Los Angeles, CA, USA, 22–24 March 2000*; p. 395.
36. Zhang, S.; Zhou, M. Stress-strain behavior of concrete-filled square steel tubes. In Proceedings of the 6th ASCCS Conference, Los Angeles, CA, USA, 22–24 March 2000; pp. 403–409.
37. Tomii, M.; Sakino, K. Experimental studies on the ultimate moment of concrete filled square steel tubular beam-columns. *Trans. Archit. Inst. Jpn.* **1979**, *275*, 55–65. [CrossRef] [PubMed]

38. Grauers, M. *Composite Columns of Hollow Steel Sections Filled with High Strength Concrete*; Chalmers University of Technology: Gothenburg, Sweden, 1993.
39. Inai, E.; Sakino, K. Simulation of flexural behavior of square concrete filled steel tubular columns. In Proceedings of the 3rd Joint Technical Coordinating Committee Meeting, US-Japan Cooperative Research Program, Phase 5: Composite and Hybrid Structures, Hong Kong, 12–14 December 1996.
40. Nakahara, H.; Sakino, K. Axial compressive and uniform bending tests of high strength concrete filled square steel tubular columns. In Proceedings of the 5th Pacific Structural Steel Conference, Seoul, Korea; pp. 943–948.
41. Varma, A.H. *Seismic Behavior, Analysis, and Design of High Strength Square Concrete Filled Steel Tube (CFT) Columns*; Lehigh University: Bethlehem, PA, USA, 2000.
42. Lu, Y.Q.; Kennedy, D.L. *The Flexural Behaviour of Concrete-Filled Hollow Structural Sections*; 0315-1468; University of Alberta: Edmonton, AB, Canada, 1992.
43. Yamamoto, T.; Kawaguchi, J.; Morino, S. Experimental study of scale effects on the compressive behavior of short concrete-filled steel tube columns. In Proceedings of the United Engineering Foundation Conference on Composite Construction in Steel and Concrete IV (AICE). Banff, Canada, 28 May–2 June 2000; pp. 879–891.
44. Han, L.-H.; Yao, G.-H. Tests on stub columns of concrete-filled RHS sections. *J. Constr. Steelwork* **2002**, *58*, 353–372. [CrossRef]
45. Lam, D.; Williams, C.A. Experimental study on concrete filled square hollow sections. *Steel Compos. Struct.* **2004**, *4*, 95–112. [CrossRef]
46. Han, L.-H.; Yao, G.-H. Experimental behaviour of thin-walled hollow structural steel (HSS) columns filled with self-consolidating concrete (SCC). *Thin-Walled Struct.* **2004**, *42*, 1357–1377. [CrossRef]
47. Zhang, Z. *Experimental Research on Short Filled Concrete Square Steel Tube Columns under Axial Compressive Load*; Harbin University of Technology: Harbin, China, 1984.
48. Xilin, L.; YuYong, C.Y. Studies on the Behavior of Concrete-filled Rectangular Tubular Short Column: I Eexperiment. *Build. Struct.* **1999**, *10*, 008.
49. Guo, L. *Theoretical and Experimental Reearch on the Behavior of Concrete-Filled Rectangular Hollow Section Steel Tubes*; Harbin Institute of Technology: Harbin, China, 2006.
50. Liu, D.; Gho, W.-M. Axial load behaviour of high-strength rectangular concrete-filled steel tubular stub columns. *Thin-Walled Struct.* **2005**, *43*, 1131–1142. [CrossRef]
51. Liu, D.; Gho, W.-M.; Yuan, J. Ultimate capacity of high-strength rectangular concrete-filled steel hollow section stub columns. *J. Constr. Steel Res.* **2003**, *59*, 1499–1515. [CrossRef]
52. Liu, D. Tests on high-strength rectangular concrete-filled steel hollow section stub columns. *J. Constr. Steel Res.* **2005**, *61*, 902–911. [CrossRef]
53. Zaili, Y. *Conpressive Behavior of high-Strength Concrete-Filled Square and Rectangular Steel Tubes*; Harbin Institute of Technology: Harbin, China, 2001.
54. Guo, L.; Zhang, S.; Kim, W. Behaviour of concrete-filled square hollow section (SHS) steel tubes under different loading conditions. In Proceedings of the Eigth International Conference for ASCCS, Harbin, China, 12–15 August 2006; pp. 83–90.

Disclaimer/Publisher's Note: The statements, opinions and data contained in all publications are solely those of the individual author(s) and contributor(s) and not of MDPI and/or the editor(s). MDPI and/or the editor(s) disclaim responsibility for any injury to people or property resulting from any ideas, methods, instructions or products referred to in the content.